RESEARCH PAPER

Physiologically based pharmacokinetic modelling and *in vivo* [I]/K_i accurately predict P-glycoprotein-mediated drug-drug interactions with dabigatran etexilate

Yuansheng Zhao[1] and Zhe-Yi Hu[2]

[1]*The Hamner Institutes for Health Sciences, Research Triangle Park, NC, USA, and* [2]*Department of Clinical Pharmacy, College of Pharmacy, University of Tennessee Health Science Center, Memphis, TN, USA*

BACKGROUND AND PURPOSE

In vitro inhibitory potency (K_i)-based predictions of P-glycoprotein (P-gp)-mediated drug-drug interactions (DDIs) are hampered by the substantial variability in inhibitory potency. In this study, *in vivo*-based [I]/K_i values were used to predict the DDI risks of a P-gp substrate dabigatran etexilate (DABE) using physiologically based pharmacokinetic (PBPK) modelling.

EXPERIMENTAL APPROACH

A baseline PBPK model was established with digoxin, a known P-gp substrate. The K_m (P-gp transport) of digoxin in the baseline PBPK model was adjusted to K_m^i to fit the change of digoxin pharmacokinetics in the presence of a P-gp inhibitor. Then '*in vivo*' [I]/K_i of this P-gp inhibitor was calculated using K_m^i/K_m. Baseline PBPK model was developed for DABE, and the '*in vivo*' [I]/K_i was incorporated into this model to simulate the static effect of P-gp inhibitor on DABE pharmacokinetics. This approach was verified by comparing the observed and the simulated DABE pharmacokinetics in the presence of five different P-gp inhibitors.

KEY RESULTS

This approach accurately predicted the effects of five P-gp inhibitors on DABE pharmacokinetics (98–133% and 89–104% for the ratios of AUC and C_{max} respectively). The effects of 16 other P-gp inhibitors on the pharmacokinetics of DABE were also confidently simulated.

CONCLUSIONS AND IMPLICATIONS

'*In vivo*' [I]/K_i and PBPK modelling, used in combination, can accurately predict P-gp-mediated DDIs. The described framework provides a mechanistic basis for the proper design of clinical DDI studies, as well as avoiding unnecessary clinical DDI studies.

Abbreviations

$AUC_{0\to\infty}$, the AUC from time zero to infinity; $AUC_{0\to t}$, the area under concentration-time curve up to the last measured time point; AUC_R, the ratio of the area under the plasma concentration-time curve ($AUC_{0\to\infty}$) in the presence and absence of the inhibitor; CL_{int}, intrinsic clearance; C_{max}, peak plasma concentration; $C_{max, R}$, the ratio of the peak concentration in the presence and absence of the inhibitor; CES, carboxylesterase; DABE, dabigatran etexilate; DDI, drug-drug interaction; [I], the effective inhibitor concentration; OATP, organic anion-transporting polypeptide; PBPK, physiologically based pharmacokinetic modelling; P-gp, P-glycoprotein; PK, pharmacokinetics;

Introduction

The transporter protein P-glycoprotein (P-gp) affects drug pharmacokinetics by limiting oral absorption, restricting CNS penetration and promoting excretion. Drug-drug interactions (DDIs) may occur when a P-gp substrate is co-administered with other drugs that inhibit P-gp. Accurate prediction of a potential risk of DDI is of great importance both within the pharmaceutical industry and in clinical practice in order to improve the safety and efficacy of new drugs.

Dabigatran etexilate (DABE) is a P-gp substrate and the first new oral anticoagulant to become available for the prevention of stroke and systemic embolism in patients with atrial fibrillation in over 50 years (Connolly *et al.*, 2009). The orally administered prodrug DABE is absorbed in the intestine and then converted by carboxylesterase (CES) to the active moiety dabigatran (DAB) which is not a P-gp substrate) (Härtter *et al.*, 2013; Hu *et al.*, 2013). Drugs that inhibit P-gp, such as verapamil, amiodarone and quinidine, raise exposures to DAB (Härtter *et al.*, 2013).

P-gp-mediated DDIs can be predicted by either a static approach or a dynamic (physiologically based pharmacokinetic, PBPK) approach. Although the static approach for the prediction of CYP450- and organic anion-transporting polypeptide (OATP)-mediated DDIs is quite successful (Hu *et al.*, 2012; Hu, 2013), the same approach for the prediction of P-gp-mediated DDIs is only qualitative due to the high rates of false-negative (10–12%) and false-positive (40–51%) results (Fenner *et al.*, 2009; Ellens *et al.*, 2013). This is probably caused by the inaccurate estimation of [I] (the effective inhibitor concentration) and K_i (inhibition constant) in the prediction of P-gp-mediated DDIs. Studies using the dynamic approach are very limited. Recently, a PBPK approach for the prediction of DDI between the P-gp substrate digoxin and verapamil was introduced (Neuhoff *et al.*, 2013b) and the predicted AUC ratio of digoxin following administration of verapamil was 1.20, while the observed value was 1.50. The verapamil K_i values considered in this study ranged from 0.1 to 16.3 (eight values from different references). The authors used the lowest K_i values for the worst-case scenario. Underestimation of the DDI will occur when other K_i values were considered. The success of this approach is dependent on the accuracy of the *in vitro* K_i used. Recently, a collaborative study was initiated between 23 pharmaceutical and contract research laboratories and one academic institution to compare *in vitro* IC$_{50}$ data generated using four *in vitro* systems (Caco-2, MDCKII-MDR1, LLC-PK1-MDR1 cells and membrane vesicles) and six transport activity equations (Bentz *et al.*, 2013). Unfortunately, the difference in IC$_{50}$ values for each of the 16 inhibitors across all test systems ranged from a minimum of 20- to 24-fold between lowest and highest IC$_{50}$ values for sertraline and isradipine, to a maximum of 407- and 796-fold for telmisartan and verapamil respectively. Further analysis showed that variability in IC$_{50}$ values was mainly due to inter-laboratory variability, rather than the systematic difference between test systems. Such substantial variability will seriously decrease the accuracy of prediction of DDIs. For example, the *in vitro* IC$_{50}$ value from some laboratories may predict significant DDI, whereas others may either over- or underestimate a DDI.

Therefore, the major challenge for the prediction of P-gp-mediated DDIs is how to identify or obtain the 'true' K_i value, which is a key input for both the static and dynamic approach. In order to overcome this difficulty, we have used the information from a typical P-gp-mediated DDI (between the P-gp substrate digoxin and a particular P-gp inhibitor) to calculate the 'in vivo' [I]/K_i for this P-gp inhibitor based on a PBPK approach. Then the 'in vivo' [I]/K_i was incorporated into the PBPK model of a test P-gp substrate (DABE) to simulate the DDI risk of DABE with this P-gp inhibitor. Our prediction method can be seen as a 'static' approach because the effective inhibitor concentration [I] in the inhibiting site is kept unchanged. This assumption is reasonable if the primary site of inhibition is in the intestine during oral absorption. We found that the elimination half-life and renal clearance of P-gp substrates such as digoxin and fexofenadine, were hardly altered by an inhibitor (Yasui-Furukori *et al.*, 2005; Tateishi *et al.*, 2008; Härtter *et al.*, 2013), suggesting the DDIs occur mainly in the intestine during the absorption process. Indeed, there were only minimal DDI risks when intravenous digoxin was given together with P-gp inhibitors (Fenner *et al.*, 2009).

The primary aim of this study was to develop an 'in vivo' [I]/K_i- and PBPK modelling-based approach for the quantitative prediction of P-gp-mediated DDIs with DABE. The approach was verified by the known effects of five different P-gp inhibitors on DABE pharmacokinetics. After that, the verified approach was used to predict the effects of 16 other P-gp inhibitors that had not been studied, on the pharmacokinetics of DABE.

Methods

Development of the PBPK model

Modelling workflow. A workflow describing the model building and validation processes that were applied to the development of the PBPK model is outlined in Figure 1. The details are described as follows:

(i) PBPK models for the orally administered P-gp substrates, digoxin and DABE (including its metabolite DAB), were constructed using *in vitro* and *in silico* data (Bottom-up), as well as the observations in a set of PK studies (Top-down). The model building strategy by Neuhoff *et al.* (2013a) was used here with some modifications.

(ii) The developed PBPK models were validated by a set of independent validation PK studies, including different doses, multiple doses, intravenous dosing or drug interaction data (P-gp-mediated induction). The major purpose of this step is to verify the contribution of passive and active efflux (P-gp) in the absorption of the studied P-gp substrates.

(iii) A reported DDI between the typical P-gp substrate (digoxin) and an inhibitor is used as the learning set. Assuming competitive inhibition, the K_m value of digoxin in the baseline PBPK model was adjusted to K_m^i to fit the change of digoxin AUC in the presence of a P-gp inhibitor. For competitive inhibition, intrinsic clearance of P-gp-mediated efflux (digoxin) in the
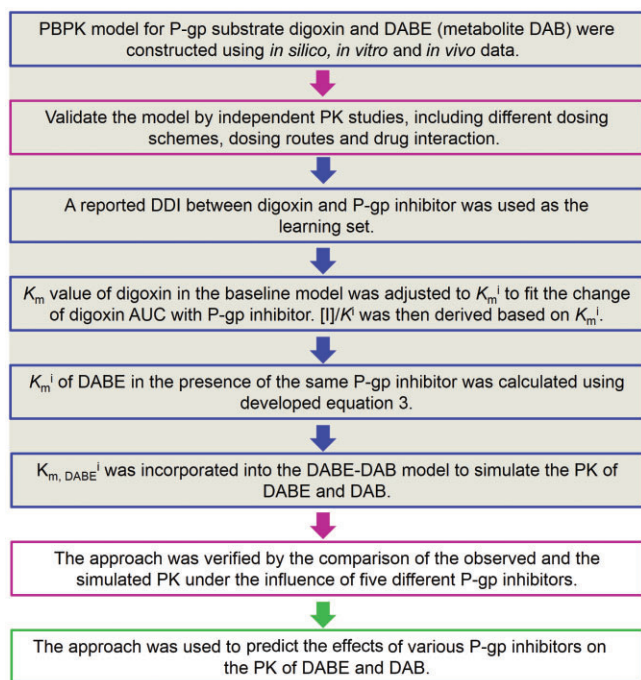
Figure 1

Workflow describing the model building and validation processes that were applied to the development of the '*in vivo*' K_i- and physiologically based pharmacokinetic modelling-based approach for the prediction of P-glycoprotein (P-gp)-mediated drug-drug interactions involving dabigatran etexilate (DABE) and its active metabolite dabigatran (DAB).

presence of inhibition (CL_{int}^i) can be calculated using equation 1, which is under first order conditions (Rowland and Matin, 1973).

$$CL_{int}^i = V_{max}/K_{m,DI}^i = \frac{V_{max}/K_{m,DI}}{1+[I]/K_i} \qquad (1)$$

where V_{max} is the maximum rate of reaction. $K_{m,\,DI}$ is the Michaelis–Menten constant for digoxin without inhibition. $K_{m,DI}^i$ is the Michaelis–Menten constant for digoxin in the presence of inhibition. [I] is the effective inhibitor concentration. K_i is the inhibition constant. Equation 2 can be derived from equation 1.

$$[I]/K_i = K_{m,DI}^i/K_{m,DI} - 1 \qquad (2)$$

Therefore, [I]/K_i of this particular P-gp inhibitor can be calculated using equation 2. It should be noted that [I]/K_i is purely derived from *in vivo* information and can been seen as the *in vivo* [I]/K_i (compared with the *in vitro* measured [I]/K_i).

(iv) A DDI between DABE and the same inhibitor is used as the test set. K_m^i of DABE in the presence of the same inhibitor is calculated using equation 3. As shown in this equation, we need not know the actual K_i of an inhibitor to calculate the K_m^i of DABE.

$$K_{m,DABE}^i = (k[I]/K_i + 1) \times K_{m,DABE} = [k(K_{m,DI}^i/K_{m,DI} - 1) + 1] \times K_{m,DABE}$$

$$(3)$$

where k is the correction factor to compensate for the dose differences of this P-gp inhibitor between the learning set and test set ($k = 1$, if the same dose is used). Then the calculated K_m^i was incorporated into the PBPK model of DABE to simulate the PK of DABE and DAB.

(v) The approach was verified by the comparison of the observed and simulated PK in the presence of five different P-gp inhibitors. The verified approach was finally used to predict the effects of various P-gp inhibitors on the PK of DABE and DAB.

Model structure and parameterization. The PBPK models for digoxin, DABE (incorporating its metabolite DAB) were built using the commercial software tool, PK-Sim® (version 5.1; Bayer Technology Services GmbH, Leverkusen, Germany), which implements a whole-body PBPK model consisting of 15 organs. The PBPK models of DABE and DAB were exported to MoBi (version 3.1; Bayer Technology Services GmbH), where they were linked to build the coupled parent-metabolite model.

All PBPK models described in the following assume an average 30-year-old white man with a body weight of 78 kg and a height of 177 cm. Physiological parameters describing basic model structure such as organ volumes, organ weights, tissue composition, blood flow rates or gastrointestinal physiology are provided within the software. The key measured and predicted input data for digoxin, DABE and DAB are listed in Table 1.

A detailed model for GI transit and absorption was used (Thelen *et al.*, 2011; 2012). In this model, the alimentary canal from the stomach to the rectum is divided into 12 compartments, each representing a definite segment of the GI tract. Intestinal permeability was calculated from the drug's lipophilicity and effective molecular weight.

The PK-Sim standard distribution model was used, which assumes four subcompartments per organ, for example, compartments for blood cells, plasma, interstitial space and cellular space. This model type considers a permeation barrier between blood and organ tissue. The rates of permeation across the cell membranes (interstitial-cell barrier) depend on the drug-specific cellular membrane permeability and the surface area available of each organ. The cellular membrane permeability values were calculated using the 'PK-Sim Standard' method. Tissue/plasma partition coefficients were generated using the model of Rodgers and Rowland (Rodgers *et al.*, 2005; Rodgers and Rowland, 2006; 2007).

Disposition characteristics of digoxin and DABE in humans. Digoxin is a P-gp substrate without the confounding effects of metabolism. P-gp plays a predominant role in the absorption and elimination of digoxin *in vivo* (Fenner *et al.*, 2009). Currently, there is no published evidence showing that digoxin is transported by any other drug transporter. The transportation of digoxin by P-gp was modelled based on Michaelis–Menten kinetics. The relative gene expression data of P-gp was integrated in the PBPK models (Meyer *et al.*, 2012). According to

Table 1

In silico, in vitro and *in vivo* data for parameterization of the physiologically based pharmacokinetic (PBPK) models for digoxin, dabigatran etexilate (DABE) and its active metabolite dabigatran (DAB)

Parameter	Digoxin Initial	Digoxin Refined	DABE Initial	DABE Refined	DAB Initial	DAB Refined
LogP	1.26 (1)	NA	3.80 (2)	NA	−2.2 (3)	NA
Molecular weight	781	NA	627	NA	471	NA
Fraction unbound in plasma (f_u)	0.71 (1)	NA	0.07[a]	NA	0.65 (4)	NA
pKa	NA	NA	4.0 (base), 6.7 (base) (2)	NA	4.1 (base), 4.4 (acid), 12.4 (base) (3)	NA
Aqueous solubility (mg mL^{-1})	0.024 (1)	1.0[b]	1.8 (2)	NA	17 (3)	NA
Human blood: plasma ratio	0.83	NA	3.08	NA	0.67 (5)	NA
Cellular (organ) permeability (nm s^{-1})	0.39	1.33	498	667	0.003	1.0
Intestinal permeability (nm s^{-1})	0.005	0.008	4.33	0.08	NA	NA
Renal clearance (mL min^{-1} kg^{-1})	2.2	1.1	NA	NA	1.63 (4)[c]	NA
Total hepatic clearance (mL min^{-1} kg^{-1})	NA	NA	NA	NA	0.41 (4)[c]	NA
CES1 metabolism						
CES1 concentration (µmol L^{-1})	NA	NA	1.0	1.59	NA	NA
V_{max} (µmol min^{-1} L^{-1})	NA	NA	NA	80	NA	NA
K_m (µM)	NA	NA	34[d]	70	NA	NA
P-gp transport						
P-gp concentration (µmol L^{-1})	1.0	NA	1.0	NA	NA	NA
V_{max} (µmol min^{-1} L^{-1})	NA	20	NA	10	NA	NA
K_m (µM)	177 (1)	NA	NA	1.0	NA	NA
Specific binding						
K_{off}	NA	0.001	NA	NA	NA	NA
K_d	NA	0.01	NA	NA	NA	NA

If not indicated, the input data were calculated by PK-Sim or was the default value in PK-Sim. The refined values were obtained by fitting the simulated plasma concentration-time profiles with the observed ones. V_{max}, maximum rate of reaction; K_m, Michaelis–Menten constant; K_{off}, dissociation rate constant; K_d, dissociation constant; NA, not applicable. The unit for the specific V_{max} used in the simulation is µmol min^{-1} L^{-1} (referring to the cellular volume).

[a]f_u of DABE is calculated using SimCYP ADME Calculators (http://www.simcyp.com/ProductServices/FreeADMETools).

[b]According to the study by Neuhoff *et al.* (2013a), the formulations currently on the market sufficiently increase the solubility.

[c]Unchanged dabigatran in urine accounted for about 80% of the i.v. dose of dabigatran (Blech *et al.*, 2008). Renal clearance was calculated by multiplying the total intravenous clearance (155 mL min^{-1}) by 80%. The remaining 20% of total clearance was attributed to hepatic clearance.

[d]From DABE enzyme kinetic studies in human liver S9 (Laizure *et al.*, 2013).

References (1), Neuhoff *et al.*, 2013a; (2), http://files.boehringer.com.au/files/PI/Pradaxa%20PI.pdf; (3), http://www.accessdata.fda.gov/drugsatfda_docs/nda/2010/022512orig1s000ea.pdf; (4), Blech *et al.*, 2008; (5), http://www.fda.gov/downloads/AdvisoryCommittees/CommitteesMeetingMaterials/Drugs/CardiovascularandRenalDrugsAdvisoryCommittee/UCM247244.pdf.

this expression data, P-gp was expressed extensively in the body including intestine, kidney and liver. Therefore, the involvement of P-gp in the hepatic and renal clearance was also considered. Renal excretion (renal clearance) was considered as the only excretion route for the elimination of digoxin in humans (Neuhoff *et al.*, 2013a). As with methotrexate (Bischoff *et al.*, 1971) and docetaxel (Bradshaw-Pierce *et al.*, 2007), specific binding to tissue components was included. This was justified by the finding that receptor (Na$^+$/K$^+$-ATPase) binding was the rate-limiting step for the distribution of digoxin (Weiss, 2007). Plasma levels of digoxin were influenced by the changes in capacity and/or affinity of digoxin binding to sodium pumps *in vivo* (Weiss, 2007). Two

parameters, K_{off} (dissociation rate constant, 1 min^{-1}) and K_d (dissociation constant, µmol L^{-1}) were introduced to express the nonlinear binding within tissue. The addition of a nonlinear binding term not only makes the model more relevant to the biochemical process in the body, but also resulted in better prediction.

The oral prodrug DABE, which is a P-gp substrate, was converted by CES enzymes to the active moiety DAB, which is not a P-gp substrate (Hu *et al.*, 2013). DAB was formed primarily in the liver by CES1 (Laizure *et al.*, 2013). Therefore, only hepatic CES1 was assumed to mediate the formation of DAB during first-pass metabolism. The relative gene expression data of CES1 is used in the PBPK models. The conversion

of DABE to DAB by CES1 and the efflux of DABE by P-gp were both modelled using Michaelis–Menten kinetics. Renal excretion (renal clearance) and hepatic metabolism (hepatic clearance) were considered as the elimination pathways of DAB from the body (Blech *et al.*, 2008).

PK data analysis

PK parameters were determined by a non-compartmental method using the Kinetica 5.0 (Thermo Fisher Scientific; Philadelphia, PA, USA). The area under the concentration-time curve up to the last measured time point ($AUC_{0 \to t}$) was calculated using the trapezoidal method. The AUC from time zero to infinity ($AUC_{0 \to \infty}$) was generated by extrapolating the $AUC_{0 \to t}$ to infinity using the elimination rate constant and the last measured concentration. All the human *in vivo* data were obtained from published data by digitalization with data mining software (GetData Graph Digitizer version 2.25, http://www.getdata-graph-digitizer.com).

Results

Simulation of DABE and DAB pharmacokinetics in humans

The predicted or assumed input data (Table 1) were refined to match the simulated plasma concentration-time profiles of

DABE and DAB with the observed data (Stangier, 2008; Stangier *et al.*, 2008; Härtter *et al.*, 2012; 2013) (Figure 2A, single oral dosing of 150 mg DABE). As shown in Figure 2B and D, the model was verified by the comparison of the simulated and observed data of multiple dosing (twice daily of 150 mg DABE) and dose-exposure relationships (Stangier *et al.*, 2007; 2012). For the dose-exposure relationships, it should be noted that the observed exposures to DAB was higher than the simulated data. This is possibly due to the different formulations that were utilized for the observed data (solution) and simulated data (capsule). In addition, there was a good agreement between the simulated [increased baseline V_{max} by 3.5 times based on the induction of P-gp expression level by rifampicin (Greiner *et al.*, 1999)] and observed exposures to DAB in the presence of the P-gp inducer rifampicin (Figure 2C). The observed ratio of DAB $AUC_{0 \to \infty}$ (AUC_R) and C_{max} ($C_{max, R}$) in the presence and absence of the inducer was 0.33 and 0.34 respectively (Härtter *et al.*, 2012). The predicted values were 0.29 and 0.28 respectively.

Simulation of digoxin pharmacokinetics in humans

The predicted or assumed input data (Table 1) were refined to match the simulated plasma concentration-time profile of
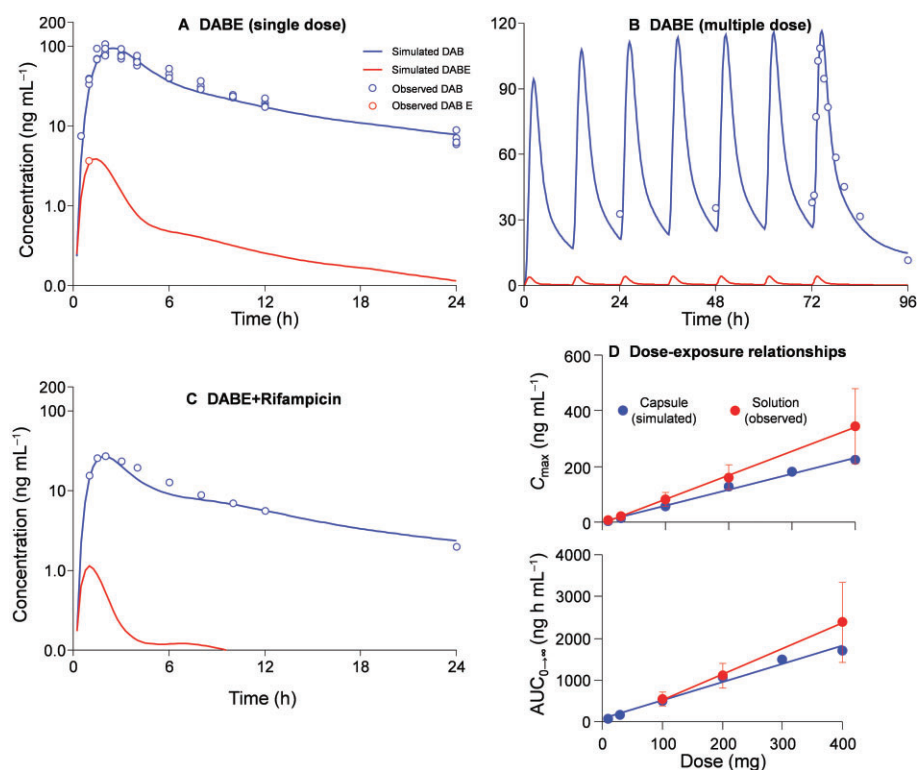

Figure 2
Simulated and observed plasma concentration-time profiles of dabigatran etexilate (DABE) and dabigatran (DAB) in human subjects after single oral dosing of 150 mg DABE (A), multiple dosing (twice daily) of 150 mg DABE (B), and co-administration of rifampicin (C, rifampicin 600 mg once daily administered for 7 days). The simulated and observed relationships between DABE doses (10 to 400 mg) and exposures to DAB (C_{max} and $AUC_{0 \to \infty}$) were also shown in panel D. For the dose-exposure relationships, the simulated data were for DABE capsule while the observed data were obtained from DABE solution. The observed data (average values) were obtained from published papers (Stangier *et al.*, 2007; 2008; 2012; Stangier, 2008; Härtter *et al.*, 2012; 2013).

digoxin with the observed data (Ragueneau *et al.*, 1999; Westphal *et al.*, 2000; Becquemont *et al.*, 2001; Verstuyft *et al.*, 2003) (Figure 3A, single oral dosing of 0.5 mg digoxin). Then the developed PBPK model was validated by the comparison of the simulated and observed data of other dose levels (single oral dosing of 0.25 mg and 1.0 mg) (Oosterhuis *et al.*, 1991; Greiner *et al.*, 1999; Eckermann *et al.*, 2012)

(Figure 3B and C). Good agreement was also observed between simulated and observed data from multiple dosing regimens (oral 0.25 mg once daily and twice daily) (Rodin *et al.*, 1988; Vaidyanathan *et al.*, 2008) (Figure 3D and E). With regard to the intravenous dosing, the simulated data and the observed data are very close (Kramer *et al.*, 1979; Ding *et al.*, 2004) (Figure 3F and G).
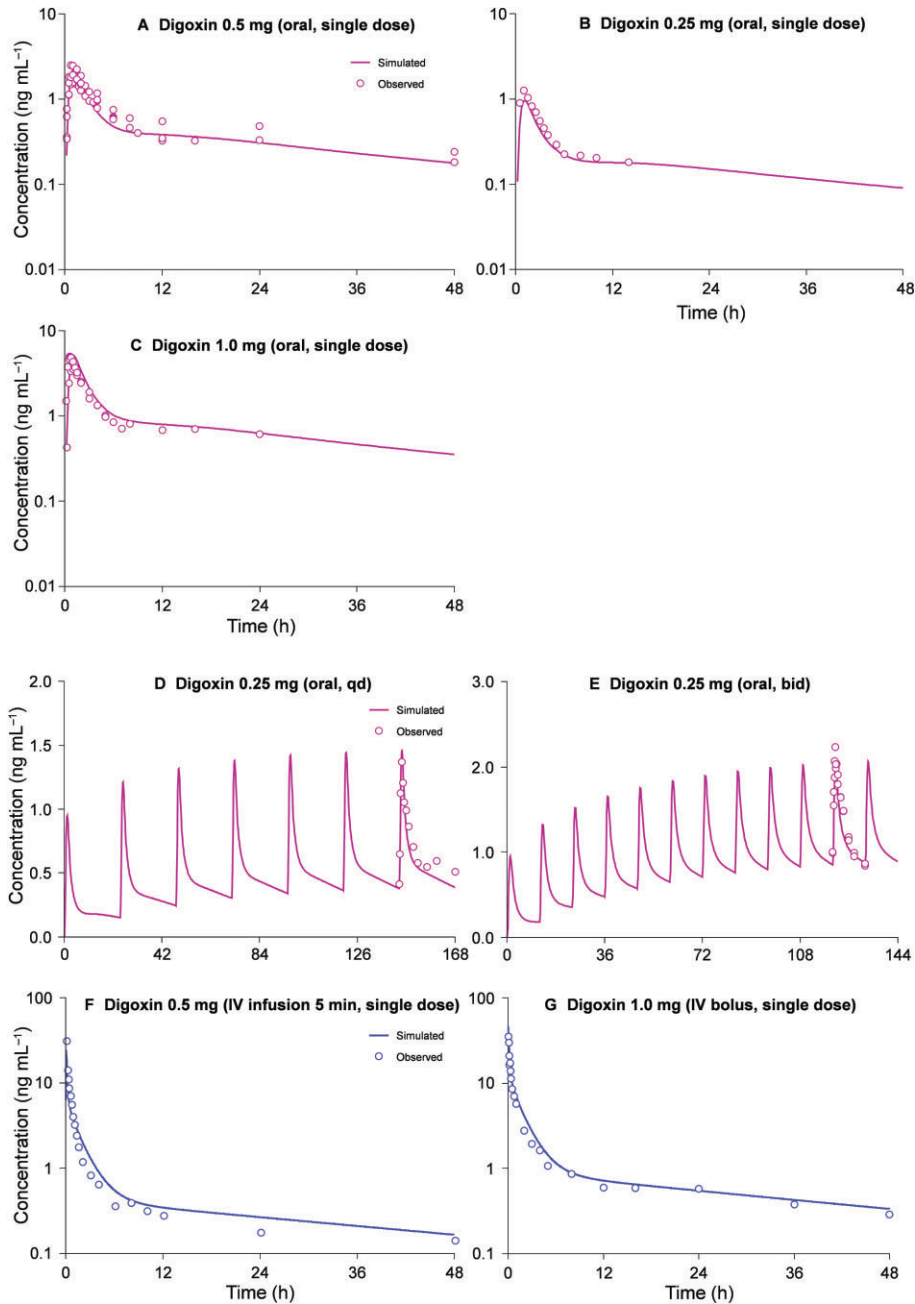

Figure 3

Simulated and observed plasma concentration-time profiles of digoxin in humans after dosing of digoxin. A, single oral dosing of 0.5 mg digoxin; B, single oral dosing of 0.25 mg; C, single oral dosing of 1.0 mg. D, oral administration of 0.25 mg digoxin once daily; E, oral administration of 0.25 mg digoxin twice daily; F, intravenous infusion of 0.5 mg digoxin over 5 min; G, intravenous bolus of 1.0 mg digoxin. The observed data (average values) were obtained from published papers (Kramer *et al.*, 1979; Rodin *et al.*, 1988; Oosterhuis *et al.*, 1991; Greiner *et al.*, 1999; Ragueneau *et al.*, 1999; Westphal *et al.*, 2000; Becquemont *et al.*, 2001; Verstuyft *et al.*, 2003; Ding *et al.*, 2004; Vaidyanathan *et al.*, 2008; Eckermann *et al.*, 2012).
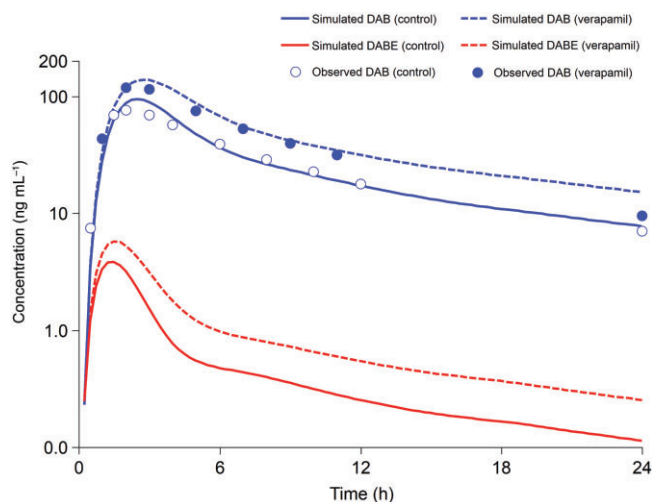
Figure 4

Simulated and observed plasma concentration-time profiles of dabigatran etexilate (DABE) and dabigatran (DAB) in human subjects after single oral dosing of 150 mg DABE with or without co-administration of verapamil (120 mg twice daily) (Härtter *et al.*, 2013).

Calculation of the 'in vivo' [I]/K_i

The calculated '*in vivo*' [I]/K_i (calculated using equation 3) of various P-gp inhibitors are shown in Supporting Information Table S1. The values of these '*in vivo*' [I]/K_i were dependent on the doses of the inhibitors. K_m^i values of DABE ($K_{m,DABE}^i$, calculated using equation 3) in the presence of various P-gp inhibitors are also shown in Supporting Information Table S1.

Comparison of the observed and simulated exposure to DAB in the presence of five P-gp inhibitors

As shown in Figure 4, there was a good agreement between the predicted and observed plasma concentration-time profile of DAB in the presence of verapamil. Positive DDIs between five P-gp inhibitors (amiodarone, clarithromycin, dronedarone, quinidine, verapamil) and DABE were reported. Our new '*in vivo*' K_i-based PBPK approach successfully predicted these DDI risks. The predictive accuracy for AUC_R and $C_{max, R}$ ranged from 98–133% to 89–104% respectively (Table 2).

Predicting the DDI risks between various P-gp inhibitors and DABE

The potential DDI risks between all the other reported P-gp inhibitors and DABE were predicted (Table 2). AUC_R and $C_{max, R}$ of DAB ranged from 1.19–1.96 to 1.13–1.57 respectively (Table 2).

Discussion

The major finding of the present study is that '*in vivo*' [I]/K_i can be used for the quantitative prediction of P-gp-mediated

DDIs. Accurate prediction of P-gp-mediated DDIs (involving DABE) was achieved when the '*in vivo*' [I]/K_i was used in combination with the PBPK modelling. The other finding is that exposure to DAB in humans is sensitive to P-gp inhibition. Identification of this class of DDIs is essential for the improvement in benefit-risk data for DABE, given the post-marketing reports of bleeding with the use of DABE (Southworth *et al.*, 2013).

Currently, only one PBPK approach for the prediction of DDI between P-gp substrate (digoxin) and inhibitor (verapamil) has been reported (Neuhoff *et al.*, 2013b). Our approach is simpler than the approach by Neuhoff *et al.* (2013b), which involved complex, dynamic DDI simulations, and metabolite inhibition potential was dynamically considered. Our prediction method can be seen as a special 'static' approach because the effective inhibitor concentration [I] is kept unchanged. However, unlike the usual static approach, our special 'static' method is still able to simulate the complete plasma concentration-time profile of the substrate drug in the presence of an inhibitor.

Simplicity has been the biggest challenge for the PBPK community to face: can such predictions be made without going through complex model building? In this study, we took a hybrid approach using substrate PBPK model and *in vivo* DDI data to define the [I]/K_i term for each inhibitor. There is, however, a simplified form of our approach. We can simply use the equation $AUC_R = 1 + [I]/K_i$ to calculate [I]/K_i, and then adjust [I]/K_i to compensate for the dose differences of this P-gp inhibitor before predicting the AUC_R for DAB with the same equation. However, there is an important assumption underlying this simplified approach. For example, the relative contribution of P-gp-mediated clearance to total clearance is the same for the substrates in the learning set (digoxin) and the test drug (DABE). Therefore, our simplified approach can be used only if this assumption (about the contribution of P-gp to total clearance) is valid. If the assumption is known not to be valid or if we do not know if it is valid or not, then our hybrid approach can be used.

Although this approach accurately predicts the influence of five P-gp inhibitors on DABE pharmacokinetics, it will be of interest to extend the approach to the prediction of DDIs between other P-gp substrates and inhibitors. Fexofenadine is a typical P-gp substrate (Draft Guidance/Guidance for Industry 2012). There are four P-gp inhibitors (from 21 inhibitors in Table 2) that were reported to be able to interact with fexofenadine, for example, itraconazole, verapamil, ritonavir and lopinavir/ritonavir (Yasui-Furukori *et al.*, 2005; Shimizu *et al.*, 2006; van Heeswijk *et al.*, 2006). However, fexofenadine is also an OATP substrate. The P-gp inhibitors verapamil, ritonavir and lopinavir/ritonavir are also able to inhibit OATP transporters (Cvetkovic *et al.*, 1999). Therefore, only the DDI involving fexofenadine and itraconazole can be used to test our approach. The reported $C_{max, R}$ and AUC_R of fexofenadine were 1.8 and 1.7 respectively (Shimizu *et al.*, 2006). The predicted values were 1.4 and 2.2 respectively. This result suggests that our approach can be extended to the prediction of the DDIs between other P-gp substrates and inhibitors.

Regulatory authorities are increasingly focusing on the use of PBPK modelling during regulatory review (Zhao *et al.*,

Table 2

Observed and simulated exposures to active metabolite dabigatran (DAB) in humans after co-administration of dabigatran etexilate (DABE, single oral dosing of 150 mg) and various P-gp inhibitors

Inhibitors	Inhibitor dosing schemes	Observed AUC$_R$	Simulated AUC$_R$	Accuracy (AUC$_R$)	Observed C$_{max, R}$	Simulated C$_{max, R}$	Accuracy (C$_{max, R}$)	Ref.
Validation set								
Amiodarone	600 mg, single	1.60	1.57	98%	1.50	1.36	91%	(1)
Clarithromycin	500 mg, bid	1.60	2.04	128%	1.49	1.54	104%	(2)
Dronedarone	400 mg, single	2.36	3.13	133%	2.25	2.08	92%	(1)
Quinidine	200 mg, every 2 h	1.53	1.79	117%	1.56	1.48	95%	(1)
Verapamil	120 mg, bid	1.53	1.75	114%	1.64	1.46	89%	(3)
Prediction set								
Captopril	1.25 mg, tid	NA	1.37	NA	NA	1.23	NA	NA
Carvedilol[a]	6.25 mg, bid	NA	1.19	NA	NA	1.13	NA	NA
Carvedilol[b]	6.25 mg, bid	NA	1.57	NA	NA	1.36	NA	NA
Conivaptan	40 mg, bid	NA	1.46	NA	NA	1.30	NA	NA
Diltiazem	60 mg, tid	NA	1.41	NA	NA	1.27	NA	NA
Felodipine	10 mg, bid	NA	1.19	NA	NA	1.13	NA	NA
Itraconazole	200 mg, qd	NA	1.71	NA	NA	1.44	NA	NA
Lopinavir/Ritonavir	400/100 mg bid	NA	1.92	NA	NA	1.55	NA	NA
Mibefradil	150 mg, qd	NA	1.30	NA	NA	1.20	NA	NA
Nifedipine	10 mg, tid	NA	1.25	NA	NA	1.16	NA	NA
Ranolazine	1000 mg, bid	NA	1.61	NA	NA	1.39	NA	NA
Ritonavir	200 mg, bid	NA	1.25	NA	NA	1.16	NA	NA
Saquinavir/Ritonavir	1000/100 mg, bid	NA	1.51	NA	NA	1.33	NA	NA
Telaprevir	750 mg, tid	NA	1.96	NA	NA	1.57	NA	NA
Telmisartan	120 mg, qd	NA	1.19	NA	NA	1.13	NA	NA
Ticagrelor	400 mg, qd	NA	1.25	NA	NA	1.16	NA	NA
Tipranavir/Ritonavir	500/200 mg, single	NA	1.79	NA	NA	1.48	NA	NA

AUC$_R$, the ratio of the area under the plasma concentration–time curve (AUC$_{0\to\infty}$) in the presence and absence of the inhibitor; C$_{max, R}$, the ratio of the peak concentration in the presence and absence of the inhibitor. qd, once daily; bid, twice daily; tid, three times a day; single, single dosing; multiple, multiple dosing; NA, not applicable.
[a]Data for the female subjects;[b] data for the male subjects.
References (1), http://files.boehringer.com.au/files/PI/Pradaxa%20PI.pdf; (2), Delavenne et al., 2013; (3), Härtter et al., 2013.

2011). Our newly developed approach was utilized to predict, with confidence, a large number of DDIs between DABE and various P-gp inhibitors that have not been studied. Based on these prediction results (Table 2), the potentially unfavourable exposure of real patients can be minimized, unnecessary clinical studies can be avoided and the study design of the clinical study can be optimized. Although [I]/K_i derived from this work may be platform-specific and would require re-parameterization when other platforms were to be used, the data of '*in vivo*' [I]/K_i (Table 2) can serve as an important database for other researchers. According to a very recent study, the '*in vivo*' inhibition potency of probenecid on renal secretion was derived using PBPK modelling (Hsu *et al.*, 2013). The authors suggested that this *in vivo* data can be used to provide an initial estimate of AUC_R values in the presence of probenecid.

In order to improve decision making in drug development and discovery, our approach can be used during the course of new drug development and discovery. If a new molecular entity is a substrate for P-gp and the PBPK model of this drug has already been established, the DDI between this drug and various P-gp inhibitors can be predicted. Our approach can reasonably exclude clinical DDI studies that later turn out to be unnecessary.

However there are limitations to the current study that need to be considered. The major challenge for the application of our approach is the accurate definition of the contribution of the P-gp transporter (to total PK) when a PBPK model for new molecular entity is being constructed. As *in vivo* clinical data were used to estimate the [I]/K_i value which was subsequently used for DAB, extrapolation outside the studied population and the conditions of the learning data set could sometimes not be justifiable. Care should be taken as the estimated parameter value might not hold in another population, with different ethnicities, P-gp genotypes or disease conditions.

In conclusion, '*in vivo*' [I]/K_i and PBPK modelling can be used in combination for the quantitative prediction of P-gp-mediated DDIs. To our knowledge, this is the first proof-of-concept study demonstrating that '*in vivo*' [I]/K_i is a useful parameter for the prediction of DDIs associated with P-gp substrates. The described general framework can be used in the course of new drug development to provide a mechanistic basis for proper design of clinical DDI studies, as well as avoiding unnecessary clinical DDI studies.

Acknowledgement

Conflict of interest

The authors declare no actual or potential conflicts of interest.

References

Becquemont L, Verstuyft C, Kerb R, Brinkmann U, Lebot M, Jaillon P *et al.* (2001). Effect of grapefruit juice on digoxin pharmacokinetics in humans. Clin Pharmacol Ther 70: 311–316.

Bentz J, O'Connor MP, Bednarczyk D, Coleman J, Lee C, Palm J *et al.* (2013). Variability in P-glycoprotein inhibitory potency (IC50) using various in vitro experimental systems: implications for universal digoxin drug-drug interaction risk assessment decision criteria. Drug Metab Dispos 41: 1347–1366.

Bischoff KB, Dedrick RL, Zaharko DS, Longstreth JA (1971). Methotrexate pharmacokinetics. J Pharm Sci 60: 1128–1133.

Blech S, Ebner T, Ludwig-Schwellinger E, Stangier J, Roth W (2008). The metabolism and disposition of the oral direct thrombin inhibitor, dabigatran, in humans. Drug Metab Dispos 36: 386–399.

Bradshaw-Pierce EL, Eckhardt SG, Gustafson DL (2007). A physiologically based pharmacokinetic model of docetaxel disposition: from mouse to man. Clin Cancer Res 13: 2768–2776.

Connolly SJ, Ezekowitz MD, Yusuf S, Eikelboom J, Oldgren J, Parekh A *et al.* (2009). Dabigatran versus warfarin in patients with atrial fibrillation. N Engl J Med 361: 1139–1151.

Cvetkovic M, Leake B, Fromm MF, Wilkinson GR, Kim RB (1999). OATP and P-glycoprotein transporters mediate the cellular uptake and excretion of fexofenadine. Drug Metab Dispos 27: 866–871.

Delavenne X, Ollier E, Basset T, Bertoletti L, Accassat S, Garcin A *et al.* (2013). A semi-mechanistic absorption model to evaluate drug-drug interaction with dabigatran: application with clarithromycin. Br J Clin Pharmacol 76: 107–113.

Ding R, Tayrouz Y, Riedel KD, Burhenne J, Weiss J, Mikus G *et al.* (2004). Substantial pharmacokinetic interaction between digoxin and ritonavir in healthy volunteers. Clin Pharmacol Ther 76: 73–84.

Draft Guidance/Guidance for Industry (2012). Drug interaction studies–study Design, data analysis, implications for dosing, and labeling recommendations. Available at: http://www.fda.gov/downloads/Drugs/GuidanceComplianceRegulatoryInformation/Guidances/UCM292362.pdf (11/18/2013).

Eckermann G, Lahu G, Nassr N, Bethke TD (2012). Absence of pharmacokinetic interaction between roflumilast and digoxin in healthy adults. J Clin Pharmacol 52: 251–257.

Ellens H, Deng S, Coleman J, Bentz J, Taub ME, Ragueneau-Majlessi I *et al.* (2013). Application of receiver operating characteristic analysis to refine the prediction of potential digoxin drug interactions. Drug Metab Dispos 41: 1367–1374.

Fenner KS, Troutman MD, Kempshall S, Cook JA, Ware JA, Smith DA *et al.* (2009). Drug-drug interactions mediated through P-glycoprotein: clinical relevance and in vitro-in vivo correlation using digoxin as a probe drug. Clin Pharmacol Ther 85: 173–181.

Greiner B, Eichelbaum M, Fritz P, Kreichgauer HP, von Richter O, Zundler J *et al.* (1999). The role of intestinal P-glycoprotein in the interaction of digoxin and rifampin. J Clin Invest 104: 147–153.

Härtter S, Koenen-Bergmann M, Sharma A, Nehmiz G, Lemke U, Timmer W *et al.* (2012). Decrease in the oral bioavailability of dabigatran etexilate after co-medication with rifampicin. Br J Clin Pharmacol 74: 490–500.

Härtter S, Sennewald R, Nehmiz G, Reilly P (2013). Oral bioavailability of dabigatran etexilate (Pradaxa®) after co-medication with verapamil in healthy subjects. Br J Clin Pharmacol 75: 1053–1062.

van Heeswijk RP, Bourbeau M, Campbell P, Seguin I, Chauhan BM, Foster BC *et al.* (2006). Time-dependent interaction between lopinavir/ritonavir and fexofenadine. J Clin Pharmacol 46: 758–767.

Hsu V, de L T Vieira M, Zhao P, Zhang L, Zheng JH, Nordmark A *et al.* (2013). Towards quantitation of the effects of renal impairment and probenecid inhibition on kidney uptake and efflux transporters, using physiologically based pharmacokinetic modelling and simulations. Clin Pharmacokinet. doi: 10.1007/s40262-013-0117-y. (in press)

Hu ZY (2013). Disposition pathway-dependent approach for predicting organic anion-transporting polypeptide-mediated drug-drug interactions. Clin Pharmacokinet 52: 433–441.

Hu ZY, Parker RB, Laizure SC (2012). In vivo information-guided prediction approach for assessing the risks of drug-drug interactions associated with circulating inhibitory metabolites. Drug Metab Dispos 40: 1487–1494.

Hu ZY, Parker RB, Herring VL, Laizure SC (2013). Conventional liquid chromatography/triple quadrupole mass spectrometry based metabolite identification and semi-quantitative estimation approach in the investigation of in vitro dabigatran etexilate metabolism. Anal Bioanal Chem 405: 1695–1704.

Kramer WG, Kolibash AJ, Lewis RP, Bathala MS, Visconti JA, Reuning RH (1979). Pharmacokinetics of digoxin: relationship between response intensity and predicted compartmental drug levels in man. J Pharmacokinet Biopharm 7: 47–61.

Laizure SC, Parker RB, Herring VL, Hu ZY (2013). Identification of carboxylesterase-dependent dabigatran etexilate hydrolysis. Drug Metab Dispos. doi: 10.1124/dmd.113.054353. (in press)

Meyer M, Schneckener S, Ludewig B, Kuepfer L, Lippert J (2012). Using expression data for quantification of active processes in physiologically based pharmacokinetic modeling. Drug Metab Dispos 40: 892–901.

Neuhoff S, Yeo KR, Barter Z, Jamei M, Turner DB, Rostami-Hodjegan A (2013a). Application of permeability-limited physiologically-based pharmacokinetic models: Part I-digoxin pharmacokinetics incorporating P-glycoprotein-mediated efflux. J Pharm Sci 102: 3145–3160.

Neuhoff S, Yeo KR, Barter Z, Jamei M, Turner DB, Rostami-Hodjegan A (2013b). Application of permeability-limited physiologically-based pharmacokinetic models: Part II-prediction of p-glycoprotein mediated drug-drug interactions with digoxin. J Pharm Sci 102: 3161–3173.

Oosterhuis B, Jonkman JH, Andersson T, Zuiderwijk PB, Jedema JN (1991). Minor effect of multiple dose omeprazole on the pharmacokinetics of digoxin after a single oral dose. Br J Clin Pharmacol 32: 569–572.

Ragueneau I, Poirier JM, Radembino N, Sao AB, Funck-Brentano C, Jaillon P (1999). Pharmacokinetic and pharmacodynamic drug interactions between digoxin and macrogol 4000, a laxative polymer, in healthy volunteers. Br J Clin Pharmacol 48: 453–456.

Rodgers T, Rowland M (2006). Physiologically based pharmacokinetic modelling 2: predicting the tissue distribution of acids, very weak bases, neutrals and zwitterions. J Pharm Sci 95: 1238–1257.

Rodgers T, Rowland M (2007). Mechanistic approaches to volume of distribution predictions: understanding the processes. Pharm Res 24: 918–933.

Rodgers T, Leahy D, Rowland M (2005). Physiologically based pharmacokinetic modeling 1: predicting the tissue distribution of moderate-to-strong bases. J Pharm Sci 94: 1259–1276.

Rodin SM, Johnson BF, Wilson J, Ritchie P, Johnson J (1988). Comparative effects of verapamil and isradipine on steady-state digoxin kinetics. Clin Pharmacol Ther 43: 668–672.

Rowland M, Matin SB (1973). Kinetics of drug-drug interactions. J Pharmacokinet Biopharm 1: 553–567.

Shimizu M, Uno T, Sugawara K, Tateishi T (2006). Effects of single and multiple doses of itraconazole on the pharmacokinetics of fexofenadine, a substrate of P-glycoprotein. Br J Clin Pharmacol 62: 372–376.

Southworth MR, Reichman ME, Unger EF (2013). Dabigatran and postmarketing reports of bleeding. N Engl J Med 368: 1272–1274.

Stangier J (2008). Clinical pharmacokinetics and pharmacodynamics of the oral direct thrombin inhibitor dabigatran etexilate. Clin Pharmacokinet 47: 285–295.

Stangier J, Rathgen K, Stähle H, Gansser D, Roth W (2007). The pharmacokinetics, pharmacodynamics and tolerability of dabigatran etexilate, a new oral direct thrombin inhibitor, in healthy male subjects. Br J Clin Pharmacol 64: 292–303.

Stangier J, Stähle H, Rathgen K, Roth W, Shakeri-Nejad K (2008). Pharmacokinetics and pharmacodynamics of dabigatran etexilate, an oral direct thrombin inhibitor, are not affected by moderate hepatic impairment. J Clin Pharmacol 48: 1411–1419.

Stangier J, Stähle H, Rathgen K, Roth W, Reseski K, Körnicke T (2012). Pharmacokinetics and pharmacodynamics of dabigatran etexilate, an oral direct thrombin inhibitor, with coadministration of digoxin. J Clin Pharmacol 52: 243–250.

Tateishi T, Miura M, Suzuki T, Uno T (2008). The different effects of itraconazole on the pharmacokinetics of fexofenadine enantiomers. Br J Clin Pharmacol 65: 693–700.

Thelen K, Coboeken K, Willmann S, Burghaus R, Dressman JB, Lippert J (2011). Evolution of a detailed physiological model to simulate the gastrointestinal transit and absorption process in humans, part 1: oral solutions. J Pharm Sci 100: 5324–5345.

Thelen K, Coboeken K, Willmann S, Dressman JB, Lippert J (2012). Evolution of a detailed physiological model to simulate the gastrointestinal transit and absorption process in humans, part II: extension to describe performance of solid dosage forms. J Pharm Sci 101: 1267–1280.

Vaidyanathan S, Camenisch G, Schuetz H, Reynolds C, Yeh CM, Bizot MN *et al.* (2008). Pharmacokinetics of the oral direct renin inhibitor aliskiren in combination with digoxin, atorvastatin, and ketoconazole in healthy subjects: the role of P-glycoprotein in the disposition of aliskiren. J Clin Pharmacol 48: 1323–1338.

Verstuyft C, Strabach S, El-Morabet H, Kerb R, Brinkmann U, Dubert L *et al.* (2003). Dipyridamole enhances digoxin bioavailability via P-glycoprotein inhibition. Clin Pharmacol Ther 73: 51–60.

Weiss M (2007). Mechanistic modeling of digoxin distribution kinetics incorporating slow tissue binding. Eur J Pharm Sci 30: 256–263.

Westphal K, Weinbrenner A, Giessmann T, Stuhr M, Franke G, Zschiesche M *et al.* (2000). Oral bioavailability of digoxin is enhanced by talinolol: evidence for involvement of intestinal P-glycoprotein. Clin Pharmacol Ther 68: 6–12.

Yasui-Furukori N, Uno T, Sugawara K, Tateishi T (2005). Different effects of three transporting inhibitors, verapamil, cimetidine, and probenecid, on fexofenadine pharmacokinetics. Clin Pharmacol Ther 77: 17–23.

Zhao P, Zhang L, Grillo JA, Liu Q, Bullock JM, Moon YJ *et al.* (2011). Applications of physiologically based pharmacokinetic (PBPK) modeling and simulation during regulatory review. Clin Pharmacol Ther 89: 259–267.

Supporting information

Additional Supporting Information may be found in the online version of this article at the publisher's web-site:

http://dx.doi.org/10.1111/bph.12533

Table S1 The data of the learning set for the calculation of the '*in vivo*' [I]/K_i of various P-gp inhibitors, and K_m^i values of dabigatran etexilate (DABE, $K_{m,DABE}^i$) in the presence of various P-gp inhibitors.